Forschungszentrum Karlsruhe
in der Helmholtz-Gemeinschaft

Wissenschaftliche Berichte
FZKA 7223

Dehydration of Methanol to Dimethylether

C. Mas, E. Dinjus, H. Ederer, E. Henrich, C. Renk

Institut für Technische Chemie

April 2006

Forschungszentrum Karlsruhe
in der Helmholtz-Gemeinschaft

Wissenschaftliche Berichte
FZKA 7223

Dehydration of Methanol to Dimethylether

C. Mas, E. Dinjus, H. Ederer, E. Henrich, C. Renk

Institut für Technische Chemie

Forschungszentrum Karlsruhe, Karlsruhe
2006

Forschungszentrum Karlsruhe GmbH
Postfach 3640, 76021 Karlsruhe

Mitglied der Hermann von Helmholtz-Gemeinschaft
Deutscher Forschungszentren (HGF)

ISSN 0947-8620

urn:nbn:de:0005-072238

Abstract

Heterogeneous-catalytic dehydration of methanol was studied using γ-Al_2O_3 in a fixed-bed reactor. The experiments were carried out in a wide pressure (2 - 5 MPa) and temperature range (250 - 350°C) at two different flow rates. Based on the bimolecular Langmuir-Hinshelwood kinetics, a model in the form of elementary reactions was generated, by means of which the results can be reproduced and interpreted well. The average errors of the individual measurements between the calculated and the experimental ones were about 0.4%.

Enwässerung von Methanol zu Dimethylether

Zusammenfassung

Die katalytische Entwässerung von Methanol am γ-Al_2O_3 wurde in einem Festbett-Reaktor untersucht. Bei einer festen Anfangszusammensetzung sind die Experimente mit zwei verschiedenen Flußgeschwindigkeiten in einem breiten Druck- (2 – 5 Mpa) und Temperaturbereich (250 – 350°C) durchgeführt worden.

Auf der Basis einer bimolekularen Langmuir-Hinshelwood Kinetik wurde ein Modell in Form von elementaren Reaktionen erstellt, durch welches die Ergebnisse sehr gut reproduziert und interpretiert werden konnten.

Der mittlere Fehler der einzelnen Messungen zwischen der berechneten und der experimentellen Konzentration war ungefähr 0,4%.

1. Introduction

1.1 General

At Forschungszentrum Karlsruhe, a process for the production of synthesis gas from lignocellulosic biomass is being developed. In a first step, biomass is liquefied by fast pyrolysis, which leaves a dense slurry consisting of pyrolysis oil and pulverised char. By slurry gasification in a pressurised entrained-flow gasifier, a tar-free, raw synthesis gas is produced at high temperature and pressure. After gas cleaning and adjustment of the H_2/CO ratio, the syngas can be converted into different products using highly selective catalysts.

On the one hand, it is possible to directly produce synfuels by the well-known Fischer-Tropsch process. On the other hand, the production of organic chemicals is of interest (Biomass To Chemicals). Special aspects of this process shall be analysed and investigated. A suitable BTC basis is the biomass to methanol and, especially, the biomass to dimethylether (DME) synthesis. The different steps leading towards DME and the overall reaction shall be investigated.

The dehydration of methanol to dimethylether shall be studied over a wide temperature and pressure range. Additionally, different space velocities are used. As catalyst, a γ-Al_2O_3 powder is applied in the reactor.

1.2 DME properties and applications

Dimethylether (DME) is a non-toxic, highly flammable, colourless gas. The properties are comparable to those of liquid gases.

Table 1: Properties of DME compared to liquid gases

	DME	Propane	Butane
Boiling Point / °C	-24.9	-42.1	-0.5
Vapour Pressure (20°C) / bar	5.1	8.4	2.1
Specific Density (g,20°C) / kg/m^3	1.59	1.52	2.01
Lower Heating Value / MJ/kg	28.43	46.36	45.74
Auto Ignition (1 atm) / °C	235 - 350	470	365
Expl. – Flamm. Limit in Air / vol%	3.4 - 17	2.1 – 9.4	1.9 – 8.4

Many applications of DME exist. For example, it is used as an aerosol propellant to replace CFC and LPG propellants in deodorants or hair sprays. In the future, it may be used as an

alternative to butane or propane (see Table 1) for household purposes like cooking etc., in gas turbines for power generation, or as a hydrogen source for fuel cells. Furthermore, it is a feedstock for fuel additives and chemicals, for example, olefins (DTO), methyl acetate, and dimethyl sulphate. The most important use of DME in the future will be that of an ultra-clean diesel alternative, due to its non-polluting properties (NO_x-free) and soot-free combustion.

1.3 DME synthesis

Two process alternatives exist for DME synthesis from synthesis gas: the one-step process or the two-step process with methanol as intermediate.
The synthesis of DME from synthesis gas consists of two steps. The first step is the synthesis of methanol (1), followed by dehydration (2).

(1) $2\ CO + 4\ H_2 \rightleftarrows 2\ CH_3OH;$
$\Delta^eG = -58.0$ kJ/mol $\quad \Delta^eH = -182.2$ kJ/mol

(2) $2\ CH_3OH \rightleftarrows CH_3\text{-}O\text{-}CH_3 + H_2O;$
$\Delta^eG = -4.5$ kJ/mol $\quad \Delta^eH = -23.5$ kJ/mol

This leads to the following global reaction (3):

(3) $2\ CO + 4\ H_2 \rightleftarrows CH_3\text{-}O\text{-}CH_3 + H_2O;$
$\Delta^eG = -62.5$ kJ/mol $\quad \Delta^eH = -205.7$ kJ/mol

In case the water-gas shift reaction (4) is supported by the catalyst

(4) $CO + H_2O \rightleftarrows CO_2 + H_2;$
$\Delta^eG = -28.6$ kJ/mol $\quad \Delta^eH = -41.2$ kJ/mol

a new global reaction (5) results as

(5) $3\ CO + 3H_2 \rightleftarrows CH_3\text{-}O\text{-}CH_3 + CO_2;$
$\Delta^eG = -91.1$ kJ/mol $\quad \Delta^eH = -246.9$ kJ/mol

Research focuses on the one-step process because of its better economic efficiency. In this paper, reaction (2) will be discussed only.

1.4 DME catalysts

For the above-mentioned reactions, various catalysts are applied. To convert synthesis gas into methanol (reaction (1)), Cu/ZnO-Al_2O_3 is employed most frequently.

For the following dehydration reaction, an acidic dehydration, various catalysts were tested. Our activities focus on using the unmodified γ-Al_2O_3 for reaction (2). It is a widely available, active, and stable catalyst for the reaction of methanol to DME and reaches a very high selectivity and a good methanol conversion rate.

Admittedly, the presence of gaseous water is a problem, because active sites are blocked. Consequently, the activity decreases at the beginning of the reaction until the equilibrium is reached.

With increasing reaction temperature, the conversion of methanol increases, too. Nearly equilibrium conversion is achieved at our reaction conditions around about T = 300°C. In long-term stability tests, γ-Al_2O_3 was found to provide for a constant methanol conversion [1], [2], [3], [4]. A larger γ-Al_2O_3 surface area increases the amount of acid sites and, hence, improves the catalytic activity [5].

Another advantage of this catalyst is that it does not support the consecutive reaction to hydrocarbons, e.g. olefins, because of less strong acid sites [6]. Other experiments showed that a treatment of γ-Al_2O_3 with formaldehyde yields a better selectivity because of a decrease in strong acid sites and an increase in weak acid sites and acidity [7].

Apart from unmodified γ-Al_2O_3, numerous other catalysts were used and tested. Various experiments were carried out with H-ZSM-5. Its methanol conversion is better than that of γ-Al_2O_3 and remains constant with increasing temperature. DME selectivity decreases with time due to coke formation at the surface and the formation of olefins. By the addition of water, H-ZSM-5 is regenerated and the yield is increased due to the removal of the coke. Moreover, the influence of the SiO_2/ γ-Al_2O_3 ratio was studied. It was found that a decreasing ratio improves the DME yield due to the less strong acid sites that support olefin and coke formation [1], [3], [8], [2].

Other catalysts used were Na-H-ZSM-5 [2], [6], amorphous SiO_2/ γ-Al_2O_3 [8], SUZ-4 [9], SAPO 34 [10], [11], [12], and TiO_2/ γ-Al_2O_3; TiO_2/ ZrO_2 [8], [13].

Aluminium oxide Al_2O_3 can be produced in a variety of solid forms [14]. For example dehydration of boehmite alumina (AlO(OH)) at 300°C-500°C yields γ-Al_2O_3, at 700°C-800°C δ-Al_2O_3 , at 900°C-1000°C θ-Al_2O_3, and at 1000°C-1200°C α-Al_2O_3 . The acid catalyst γ-Al_2O_3 is a p-block metal oxide with an Al : O ratio < 2 : 3. The missing oxygen part has not yet been characterised [15]. The most stabile configuration, α-Al_2O_3, is an hcp (hexagonal-cubic package) of oxygen atoms, in which the 4th and 6th Al cations are coordinated, while γ-Al_2O_3 has an incomplete, defective Spinell structure. This means that the Al cations are distributed among four and six coordinated centres, which leads to a surface structure with variable electronic properties. These properties result in varying acid strengths, coverages of the surface, and, hence, reactivities.

1.5 Mechanism and kinetics

For the reaction of methanol to DME, various mechanisms were proposed and studied. Bandiera *et al.* [16] used the Langmuir-Hinshelwood mechanism to explain the heterogeneously catalysed surface reaction. The methanol molecules are adsorbed at two different types of sites, the acid (Lewis) and its adjacent basic site (Broensted).

The adsorption step on the proton is described as

$$CH_3OH + H^+ \rightleftarrows [CH_3{\cdot}OH_2]^+ \quad (6)$$

Simultaneously, the methanol molecules are adsorbed on the basic site:

$$CH_3OH + O^{2-} \rightleftarrows [CH_3{\cdot}O]^- + [OH]^- \quad (7)$$

These two surface species then form DME by condensation.

$$[CH_3{\cdot}OH_2]^+ + [CH_3{\cdot}O]^- \rightleftarrows CH_3\text{-}O\text{-}CH_3 + H_2O \quad (8)$$

The catalyst surface regenerates by the following reactions

$$H_2O + [OH]^- \rightleftarrows [H_3O]^+ + O^{2-} \quad (9)$$

$$[H_3O]^+ \rightleftarrows H_2O + H^+ \quad (10)$$

As catalyst, an H-mordenite zeolite was used in this case. Measurements took place at atmospheric pressure and temperatures between 200°C and 300°C.

Another mechanism was mentioned by Kubelková *et al.* [17]. Here, only one methanol molecule is adsorbed on the surface with a transition of a H^+ proton. After dehydration, a

methoxyl group remains on the surface. Another methanol molecule reacts with the methoxyl group to DME.

$$CH_3OH\ (ads) \rightleftarrows CH_3OH_2^+ \rightleftarrows —CH_3 + H_2O \qquad (11)$$

$$—CH_3 + CH_3OH \rightleftarrows CH_3\text{-}O\text{-}CH_3 + —H \qquad (12)$$

In this case, HY and HZSM-5 zeolites were used as catalysts at atmospheric pressure and temperatures of 400°C.

Blaszkowski *et al.* [18] theoretically studied both mechanisms. According to calculation, the mechanism suggested by Bandiera *et al.* [16] is more favourable from the energetic point of view.

A special study of the intrinsic kinetics of methanol dehydration to DME on a γ-Al_2O_3 catalyst was accomplished by Berčič *et al.* [19]. Assuming the surface reaction to be the rate-controlling step and the Langmuir-Hinshelwood mechanism to apply, the following expression is obtained for the rate equation:

$$-r_M = \frac{k_S K_M^2 \left(C_M^2 - C_W C_D / K\right)}{\left(1 + 2\left(K_M C_M\right)^{1/2} + K_W C_W\right)^4} \qquad (13)$$

$-r_M$	-	reaction rate	/ mol/(g_{cat}/h)
k_S	-	rate constant of surface reaction	/ mol/(g_{cat}/h)
K_i	-	adsorption constant	/ m^3/kmol
C_i	-	concentration	/ kmol/m^3
K	-	equilibrium constant	/ -

Equation (13) follows the Hougen-Watson rate equation.

2. Experimental

2.1 The catalyst

The γ-Al_2O_3 catalyst (MERCK, Art. No. 101095, anhydrous) has the following data:

Table 2: Chemical data of γ-Al_2O_3

Molar mass / g/mol	101.94
Density / g/cm^3	3.50 - 3.90
Bulk density / kg/m^3	972
Specific surface area / m^2/g	130

The particle size of the powder is specified as follows:

Table 3: Particle size distribution

> 0.2 mm	$\leq$ 2 %
< 0.063 mm	$\leq$ 28 %
> 0.063 mm	$\geq$ 72 %

Temperature-programmed desorption (TPD) (Micromeritics device) with ammonia revealed that 7.045 ml_{NH3}/g_{cat} (0.306 mol_{NH3}/l_{cat}) were adsorbed on the surface. At a surface area of 130 m^2/g_{cat} and a average cross-section of 0.0857 nm^2/Al_{atom}, about every 8th acid site on the surface is used as “active centre”.

2.2 Reactor system: fixed-bed reactor

The system mainly consists of 5 parts:

- A ceramic tubular flow reactor made of non-reactive Al_2O_3, surrounded by an electric heater with a removable basket to insert the catalyst.
- A gas supply line with mass flow meters and control devices.
- A control valve to set a constant pressure.
- A LiquiFlow, followed by an evaporator for water or methanol gas feeding.
- Two analytical devices (gas chromatography and mass spectroscopy).

❖ The tubular reactor with two flanges on both sides was cast in one piece by the Friatec AG company. Its total length was 400 mm. The tube surface was provided with spiral-like grooves of 1 mm depth and 1 mm width over a total length of 250 mm. The centres of the grooves were located at 2 mm distance. Into the grooves, a

heating wire (ferritic alloy: FeCrAl) made by the Kanthal company was inserted. This wire was 17 m long, had a diameter of 1 mm, and an electric resistance of 1.78 Ω/m. When operated at 110 V alternating voltage, it supplied a power of about 400 W.

The counterparts of the ceramic flanges were made of stainless steel with two inlets of 1 mm in diameter each. Via stainless steel lines, they were connected with the supply units. At the inlet flange, a ceramic rod of 170 mm length and any diameter could be screwed in to adjust an optimum gas flow in the reactor and reduce the gas inventory. The flanges were sealed by o-rings made of PTFE with 25% reinforced glass fibre and withstood temperatures of up to 250°C. The reactor was subjected to leak tests at pressures of up to 150 bar.

- Supply units:
  a) Mass flow converters (by the Wagner company) were operated up to a maximum flow rate of 100 mln/min and up to 105 bar. They were calibrated with air or N_2.
  b) The pressure control unit (by the Haenni company) was calibrated up to 100 bar and up to a maximum temperature of 300°C.
  c) LiquidFlow (by the Wagner company), maximum flow rate 5 g/h for H_2O, calibrated up to 105 bar. The downstream evaporator, (aDROP company), with a heat control unit and temperature display up to 400°C, tested up to a flow rate of 20 g/h H_2O, total power 250 W.

- Detection units:
  a) Micro gas chromatograph (Agilent company), with two columns (molecular sieve 5 Å, 12 m x 0.32 mm; PoraPak Q, 8 m X 0.2 mm) and a thermal conductivity detector. The micro GC is run isothermally with an injection time of 30 ms. An analysis run takes 160 seconds.
  b) Quadrupole mass spectometer (Pfeiffer company), with two detectors: Faraday, CHTRON, and mass range up to 300 amu.

The catalytic reaction was observed online by mass spectrometry using various output methods, e.g. multiple ionisation detection or multiple concentration detection or analogue scan presentation. The data acquisition system of Interllution Co. and home-built electronic and mechanical devices were used to record all the necessary parameters of the experimental setup and store them in an Access database.

The entire setup is represented schematically in Figure 1.

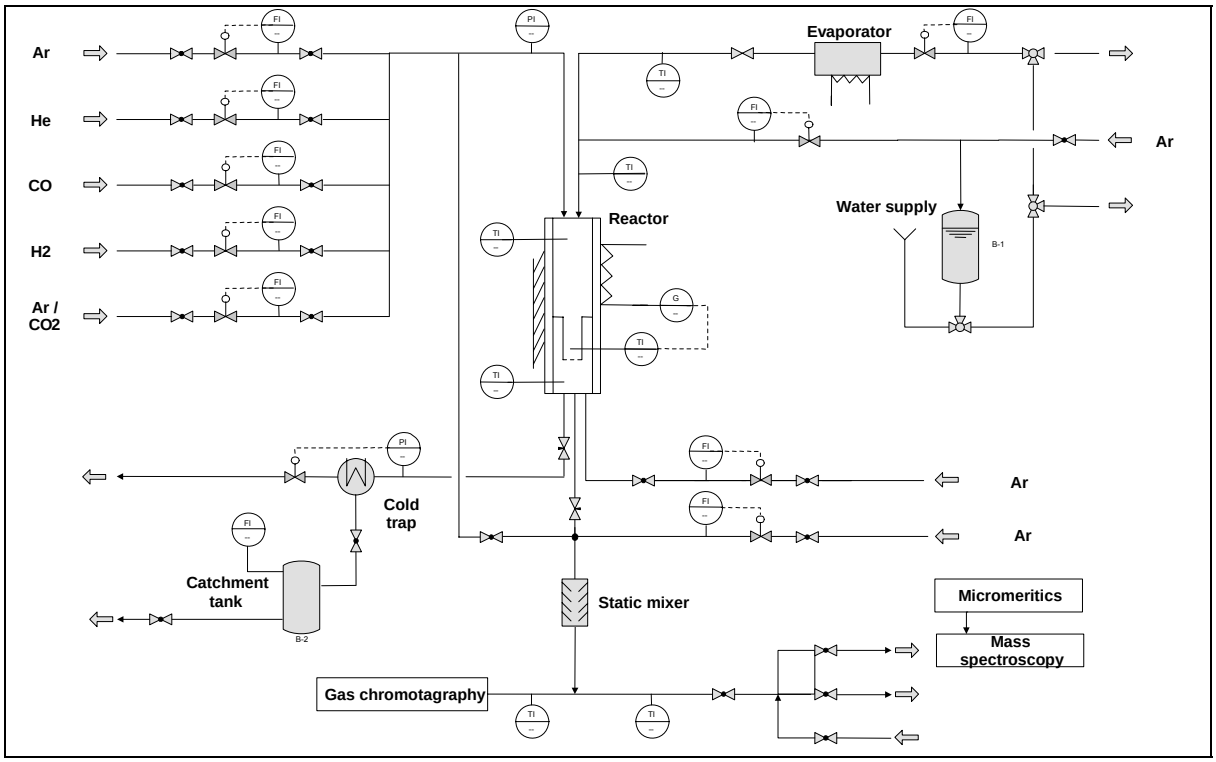

Fig. 1. Schematic representation of the entire setup.

2.3 Experiments

In total, 43 experiments were carried out. The smallest temperature selected was 250°C, as hardly any methanol was converted at temperatures below. Hence, the experiments were performed at five different temperatures in the range of 250 to 350°C, at four different pressures between 21 and 51 bar with increments of 10 bar, and at two flow rates of 54.2 and 108.4 $^{mln}/_{min.}$, respectively (mln = ml at 1013.25 mbar and 0°C). 300.7 mg catalyst were used without any activation.

Methanol concentration in the inlet gas always amounted to 18.6% (in molar units), the remainder was a mixture of Ar, N_2 and He, usually, argon (37%) + N_2 (18.4%) + He (26%). After the gases had passed the catalyst, they were diluted with argon to prevent condensation in the approximately 3 m long lines towards the detection units. The lines were heated to 120°C and manufactured specially for gas chromatography (Agilent company), above all from copper.

A gas chromatogram was recorded only when all masses were constant at the mass spectrometer (usually, after 1 to 2 hours) and when the He to N_2 ratio corresponded to the value specified.

Table 4 lists all experiments. 40 different experiments were carried out and three experiments were repeated (runs 66-67, 83-84, and 89-90).

Table 4. Summary of all experimental results

Run is the reference number of the experiment
T is the temperature in K
P is the pressure in bar
t is the formal reaction time in seconds
fch3oh is the feed concentration of CH_3OH in mol/l and in mbar
ch3oh is the concentration of CH_3OH in mol/l and in mbar after the reaction
dme is the concentration of CH_3OCH_3 (DME) in mol/l and in mbar after the reaction
h20 is the concentration of H_2O in mol/l and in mbar after the reaction
co is the concentration of CO in mol/l and in mbar after the reaction
h2 is the concentration of H_2 in mol/l and in mbar after the reaction
co2 is the concentration of CO_2 in mol/l and in mbar after the reaction

Run	T K	P bar	t s	fch3oh mol/l	fch3oh mbar	ch3oh mol/l	ch3oh mbar	dme mol/l	dme mbar	h2o mol/l	h2o mbar
58	523	51.1	2.25	0.219	9496.0	0.200	8690.4	0.005	203.2	0.005	196.1
59	548	51.1	2.14	0.208	9496.0	0.179	8146.3	0.010	472.9	0.009	432.7
60	573	51.0	2.05	0.199	9492.3	0.148	7061.2	0.021	1003.3	0.019	896.3
61	598	51.1	1.96	0.191	9494.2	0.114	5658.1	0.034	1680.5	0.030	1490.6
62	623	51.1	1.88	0.183	9496.0	0.083	4315.3	0.045	2356.2	0.042	2199.0
63	522	51.0	1.12	0.219	9492.3	0.203	8826.9	0.002	102.5	0.003	111.1
64	548	51.0	1.07	0.208	9490.5	0.185	8412.4	0.006	270.7	0.006	256.7
65	573	51.0	1.02	0.199	9492.3	0.161	7676.0	0.013	636.9	0.012	580.6
66	598	51.0	0.98	0.191	9492.3	0.132	6553.9	0.024	1168.2	0.021	1045.1
67	598	51.1	0.98	0.191	9494.2	0.132	6559.8	0.024	1169.5	0.021	1050.6
68	623	51.1	0.94	0.183	9494.2	0.105	5445.0	0.033	1708.8	0.030	1536.0
69	523	41.1	0.90	0.176	7634.4	0.164	7114.4	0.002	84.7	0.002	89.4
70	548	41.1	0.86	0.168	7636.3	0.148	6749.8	0.006	250.6	0.005	232.7
71	573	41.1	0.82	0.160	7634.4	0.130	6205.5	0.011	530.7	0.010	482.1
72	598	41.1	0.79	0.154	7634.4	0.106	5288.6	0.020	997.9	0.018	896.9
73	623	41.1	0.76	0.147	7636.3	0.084	4339.2	0.029	1477.7	0.026	1350.2
74	523	41.0	1.80	0.175	7632.5	0.153	6634.8	0.004	160.5	0.004	155.3
75	548	41.1	1.72	0.168	7634.4	0.135	6143.0	0.009	412.2	0.008	373.3
76	573	41.1	1.65	0.160	7634.4	0.111	5272.1	0.018	867.8	0.016	784.2
77	598	41.1	1.58	0.154	7636.3	0.085	4246.2	0.028	1388.7	0.025	1250.2
78	623	41.1	1.52	0.147	7636.3	0.064	3339.6	0.036	1845.4	0.034	1756.7
79	523	31.1	0.68	0.133	5780.2	0.129	5594.4	0.002	65.9	0.002	67.1
80	548	31.1	0.65	0.127	5780.2	0.119	5425.4	0.003	152.9	0.003	141.0
81	573	31.1	0.62	0.121	5778.3	0.104	4934.5	0.008	392.5	0.007	355.4

Run	T K	P bar	t s	fch3oh mol/l	fch3oh mbar	ch3oh mol/l	ch3oh mbar	dme mol/l	dme mbar	h2o mol/l	h2o mbar
82	598	31.1	0.60	0.116	5778.3	0.086	4271.9	0.015	722.4	0.013	648.6
83	623	31.1	0.57	0.112	5780.2	0.070	3606.7	0.020	1056.5	0.018	950.7
84	623	31.1	0.57	0.112	5778.3	0.070	3647.5	0.020	1035.3	0.018	947.0
85	523	31.1	1.37	0.133	5778.3	0.125	5429.0	0.003	127.6	0.003	117.8
86	548	31.1	1.30	0.127	5778.3	0.110	5007.3	0.007	324.1	0.006	290.6
87	573	31.1	1.25	0.121	5776.5	0.091	4323.5	0.014	668.9	0.013	602.1
88	598	31.1	1.20	0.116	5776.5	0.071	3531.0	0.021	1067.0	0.019	961.2
89	623	31.1	1.15	0.112	5776.5	0.055	2841.1	0.027	1413.9	0.026	1354.8
90	623	31.1	1.15	0.112	5778.3	0.055	2856.4	0.027	1410.3	0.027	1373.9
91	523	21.1	0.93	0.090	3922.3	0.085	3704.8	0.002	82.2	0.002	77.1
92	548	21.1	0.89	0.086	3922.3	0.076	3445.0	0.005	208.9	0.004	190.1
93	573	21.1	0.85	0.082	3922.3	0.063	3008.0	0.009	427.9	0.008	384.7
94	598	21.1	0.81	0.079	3922.3	0.051	2556.0	0.013	656.8	0.012	602.8
95	623	21.1	0.78	0.076	3922.3	0.043	2210.8	0.016	827.0	0.015	758.0
96	523	21.1	0.46	0.090	3920.4	0.087	3777.7	0.001	54.0	0.001	52.7
97	548	21.1	0.44	0.086	3922.3	0.080	3632.4	0.003	130.1	0.003	121.0
98	573	21.1	0.42	0.082	3922.3	0.070	3311.4	0.006	288.4	0.005	257.2
99	598	21.1	0.41	0.079	3920.4	0.061	3011.1	0.009	435.1	0.008	398.4
100	623	21.1	0.39	0.076	3920.4	0.053	2732.9	0.011	577.1	0.010	525.4
101	523	36.0	10000	0.154	6695.2	0.017	747.0	0.068	2974.1	0.068	2974.1
102	548	36.0	10000	0.147	6695.2	0.018	824.2	0.064	2935.5	0.064	2935.5
103	573	36.0	10000	0.141	6695.2	0.019	900.7	0.061	2897.3	0.061	2897.3
104	598	36.0	10000	0.135	6695.2	0.020	975.9	0.058	2859.7	0.058	2859.7
105	623	36.0	10000	0.129	6695.2	0.020	1049.6	0.054	2822.8	0.054	2822.8

The coloured lines contain the results of experiments performed at longer retention times (total flow 54.2 $^{mln}/_{min}$). The lines that are not shaded grey list the results obtained at shorter retention times (total flow 108.4 $^{mln}/_{min}$).

The last five entries of Table 4 refer to the dependence of the equilibrium values of the five experimental temperatures. These entries were calculated with the ASPEN programme at a pressure of 36 bar.

The second part of Table 4 represented below reflects the formation of CO, H_2, and traces of CO_2. At 31 and 21 bar, very small amounts of CO ($<$ 2%, with the exception of run 86 - 2.4%) and H_2 are formed. Their ratios nearly exactly correspond to ½ in all experiments. The experiments at 41 and 51 bar reveal higher conversion rates for CO (up to 9.1% - run 74). Nevertheless, formation was not found to be related to temperature. It was therefore supposed that CO is not formed in the catalyst, but outside. Later studies revealed that in the presence of H_2O, CH_3OH in Cu lines is decomposed into CO and $2H_2$ at $\geq$ 120°C already. When adding H_2O into the lines, CO was converted into CO_2 + H_2 according to the water-gas shift reaction. As a result, the CO disappeared practically completely. In addition, CH_4 was formed with a surplus of DME. For all these reasons, the CO was taken to be included in the non-converted CH_3OH.

Run	T K	P bar	t s	co mol/l	co mbar	h2 mol/l	h2 mbar	co2 mol/l	co2 mbar
58	523	51.1	2.25	0.009	399.3	0.019	841.8	0.002	88.5
59	548	51.1	2.14	0.009	404.0	0.019	876.9	0.002	77.5
60	573	51.0	2.05	0.009	424.4	0.020	951.2	0.002	76.7
61	598	51.1	1.96	0.010	474.9	0.020	992.8	0.002	78.5
62	623	51.1	1.88	0.009	468.2	0.020	1037.7	0.002	80.9
63	522	51.0	1.12	0.011	460.4	0.024	1037.5	0.002	74.0
64	548	51.0	1.07	0.012	536.7	0.024	1074.3	0.002	73.7
65	573	51.0	1.02	0.011	542.5	0.025	1211.8	0.002	76.3
66	598	51.0	0.98	0.012	602.1	0.026	1274.5	0.002	75.8
67	598	51.1	0.98	0.012	595.3	0.026	1276.4	0.002	76.5
68	623	51.1	0.94	0.012	631.5	0.026	1342.1	0.002	79.2
69	523	41.1	0.90	0.008	350.6	0.017	757.4	0.001	64.1
70	548	41.1	0.86	0.008	385.3	0.018	828.5	0.001	61.4
71	573	41.1	0.82	0.008	367.6	0.016	786.0	0.001	57.3
72	598	41.1	0.79	0.007	349.9	0.015	741.7	0.001	60.8
73	623	41.1	0.76	0.007	341.5	0.014	720.0	0.001	62.9
74	523	41.0	1.80	0.016	676.8	0.033	1444.6	0.002	79.8
75	548	41.1	1.72	0.015	666.9	0.030	1386.6	0.002	71.9
76	573	41.1	1.65	0.013	626.7	0.028	1324.8	0.001	71.4
77	598	41.1	1.58	0.012	612.6	0.026	1317.3	0.001	70.6
78	623	41.1	1.52	0.012	605.9	0.025	1292.6	0.001	74.8
79	523	31.1	0.68	0.001	53.9	0.002	101.9	0.001	36.6
80	548	31.1	0.65	0.001	49.0	0.002	88.6	0.001	30.2
81	573	31.1	0.62	0.001	58.8	0.002	113.0	0.001	36.5
82	598	31.1	0.60	0.001	61.7	0.002	116.8	0.001	37.5
83	623	31.1	0.57	0.001	60.5	0.002	114.9	0.001	38.7
84	623	31.1	0.57	0.001	60.3	0.002	115.6	0.001	38.3
85	523	31.1	1.37	0.002	94.2	0.005	198.9	0.001	41.9
86	548	31.1	1.30	0.003	122.8	0.005	223.5	0.001	42.9
87	573	31.1	1.25	0.002	115.2	0.005	230.5	0.001	43.6
88	598	31.1	1.20	0.002	111.5	0.005	225.6	0.001	41.9
89	623	31.1	1.15	0.002	107.5	0.004	222.4	0.001	43.8
90	623	31.1	1.15	0.002	101.3	0.004	213.7	0.001	44.2
91	523	21.1	0.93	0.001	53.1	0.002	106.2	0.001	29.1
92	548	21.1	0.89	0.001	59.5	0.002	103.5	0.001	27.9
93	573	21.1	0.85	0.001	58.4	0.002	100.7	0.001	27.6
94	598	21.1	0.81	0.001	52.7	0.002	97.7	0.001	28.8
95	623	21.1	0.78	0.001	57.5	0.002	97.9	0.001	28.5
96	523	21.1	0.46	0.001	34.7	0.001	61.9	0.001	25.9
97	548	21.1	0.44	0.001	29.7	0.001	57.0	0.001	24.8
98	573	21.1	0.42	0.001	34.2	0.001	54.6	0.001	26.7
99	598	21.1	0.41	0.001	39.1	0.001	55.4	0.000	24.9
100	623	21.1	0.39	0.001	33.3	0.001	62.4	0.000	25.5
101	523	36.0	10000	0.000	0.0	0.000	0.0	0.000	0.0
102	548	36.0	10000	0.000	0.0	0.000	0.0	0.000	0.0
103	573	36.0	10000	0.000	0.0	0.000	0.0	0.000	0.0
104	598	36.0	10000	0.000	0.0	0.000	0.0	0.000	0.0
105	623	36.0	10000	0.000	0.0	0.000	0.0	0.000	0.0

To obtain an impression of the conversion of methanol as a function of temperature, the results are represented graphically in Figure 2.

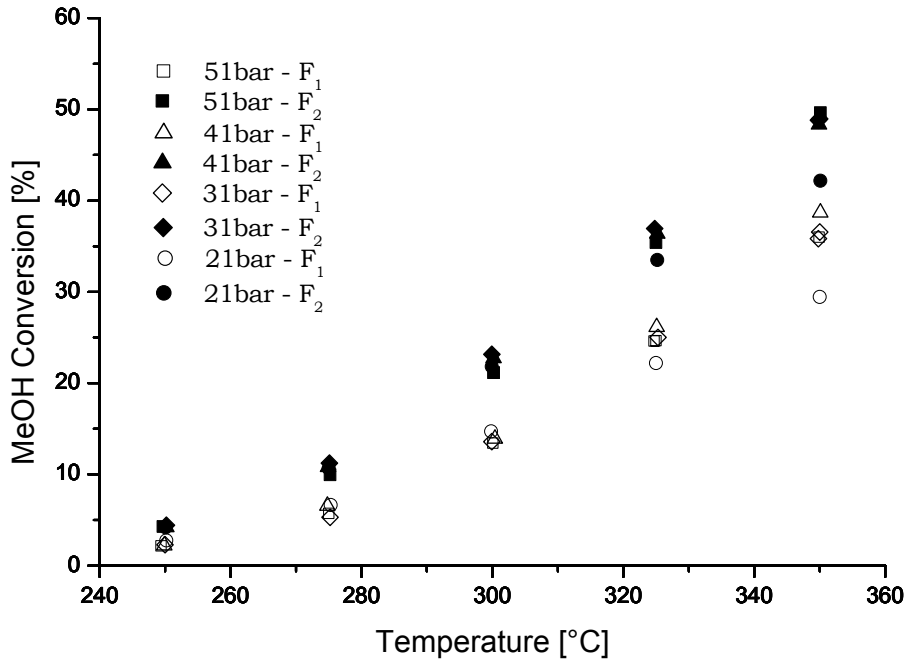

Fig. 2. Conversion of MeOH versus temperature at 4 pressures and 2 retention times. F_1 = total flow (108.4 *mln/min*), F_2 = total flow (54.2 *mln/min*).

2.4 Description of all kinetic experiments by a model based on elementary reactions

The mathematical model was described in detail in [20] by Ederer et al. when studying the water-gas shift reaction. Based on this experience, the reaction system given below was developed. It allows to calculate parameters that are relevant to the design of a pilot plant for the direct conversion of synthesis gas to DME. The decomposition of methanol may be described most easily by the following reaction system:

Table 5. Reaction mechanism for simple kinetics, including adsorption desorption kinetics

k_1 :	CH_3OH	+	Z	------>	CH_3OH^{ads}			
k_4 :	CH_3OH^{ads}			------>	CH_3OH	+	Z	
k_2 :	DME	+	Z	------>	DME^{ads}			
k_5 :	DME^{ads}			------>	DME	+	Z	
k_3 :	H_2O	+	Z	------>	H_2O^{ads}			
k_6 :	H_2O^{ads}			------>	H_2O	+	Z	
k_7 :	CH_3OH^{ads}	+	CH_3OH^{ads}	------>	DME^{ads}	+	H_2O^{ads}	
k_8 :	DME^{ads}	+	H_2O^{ads}	------>	CH_3OH^{ads}	+	CH_3OH^{ads}	

$Z_{total} = Z + Z_{CH3OH} + Z_{DME} + Z_{H2O}$ = 0.306 mol/l_{Kat}, Section **2.1** (NH_3 titration)

The following assumptions were made:

a) Transport due to diffusion or surface diffusion do not play any role
b) The chemical reaction is the rate-controlling step
c) 3 adsorption equations
d) 3 desorption equations
e) 2 chemical reactions at the surface

The square of the relative error of DME was used as objective function for the total of the error squares. The errors of the other substances corresponded to that of DME. Optimisation was carried out by means of the Simplex method implemented in MATLAB. During the model calculations of the time/conversion rate characteristics, it was always ensured that the equilibrium values were reached after longer terms.

Equation (13) was calculated in addition to the reaction system. It also considered the reverse reaction of desorption. The results obtained using equation (13) could not be distinguished from our results. The total of the error squares was worse by a factor of 2. Figures 3 and 4 show the good agreement between the calculated and experimental values.

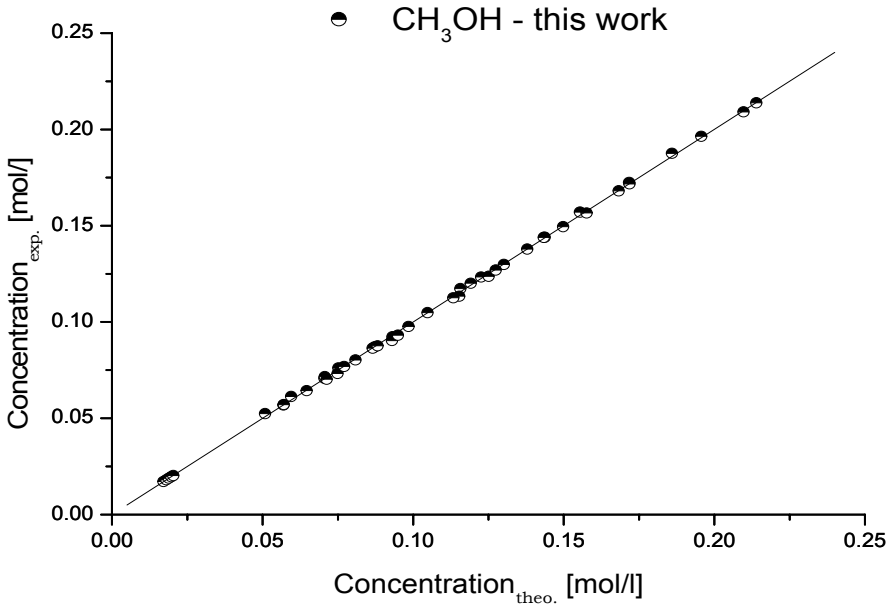

Fig. 3. Comparison of the experimental and calculated values for methanol.

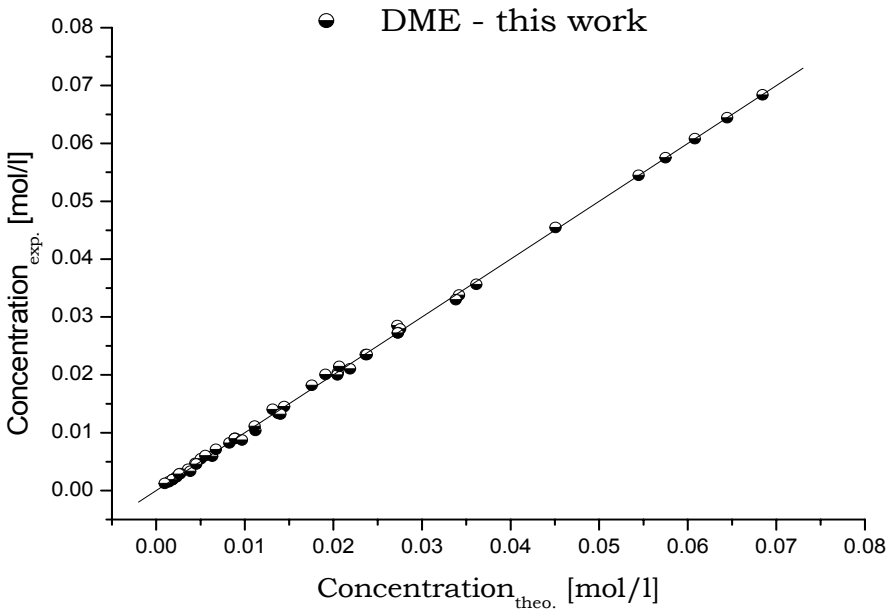

Fig. 4. Comparison of the experimental and calculated values for dimethylether.

It is obvious from Figures 3 and 4 that the start or end points are the equilibrium points. They are in agreement with the experimental values. Having this good agreement between the

experimental and theoretical values, methanol conversion may be studied as a function of an increasing methanol concentration in the feed gas. This is shown in Fig. 5.

At first, the model supplied a data set with the smallest total of error squares ($2.14*10^{-5}$). With this data set, the experimental results were reproduced well. However, the values of the pre-exponential factors strongly deviated from those given in literature. For this reason, values that appeared to be physically reasonable were entered for the optimisation run. The result was a total of error squares ($2.19*10^{-5}$) that was about 2% worse than the previous one. However, the values of the pre-exponential factors were considered to be physically reasonable and the results were reproduced well, of course. This only shows that the objective function is not the only criterion for a good representation of the results. It is also necessary to critically analyse what is physically reasonable.

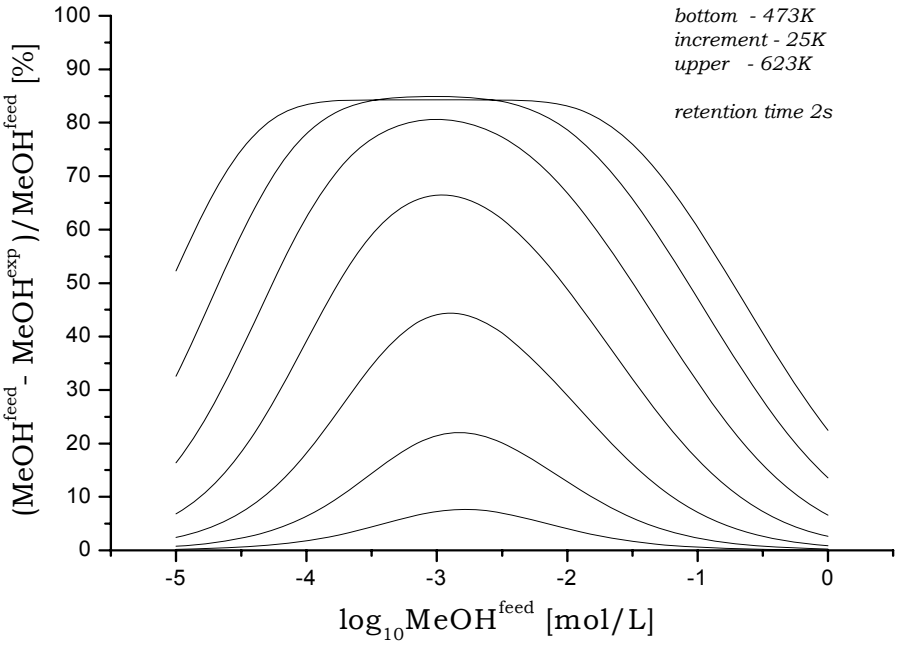

Fig. 5. Conversion as a function of the increasing methanol concentration in the feed gas.

To plot this figure and for a better understanding, the results with the ($2.14*10^{-5}$) total of error squares were used, since the temperature dependence of the various characteristics was symmetric in this case. The methanol concentration results obtained with the ($2.19*10^{-5}$) total of error squares were smaller than those shown here by four orders of magnitude (low pressure), and the characteristics were not as symmetric as those shown here.

It is obvious from the figure that the conversion rate passes a maximum. The position of this maximum depends on temperature. In this example, conversion at a retention time of 2 s increases significantly for all curves obtained at a low methanol concentration (low pressure) according to a reaction of second order. Formally speaking, this increase gradually drops down to the first order at the maximum.

At the maximum, coverage of the surface is ½ (50%). In the model, coverage follows the Langmuir isotherm. Hence, the conversion rate (degree of coverage) is proportional to the methanol feed pressure (methanol concentration), that is $(P^0_{MeOH})^{½}$. At the highest temperature, 623 K, a plateau develops. This means that the beginning of the plateau is reached when the equilibrium position is reached. This happens at $(P^0_{MeOH})^{½}$, which corresponds to a degree of coverage of ~40% in this example (T = 623 K, t = 2 s). The formal kinetics of first order are maintained when the pressure is increased until coverage of the active centres on the plateau is complete. Consequently, the conversion of DME is constant at the maximum and on the plateau.

Further increase of the pressure does not result in any further increase of the conversion rate. The conversion rates of DME and methanol approach a limit value. From the formal point of view, this is a result of the reduction of the order to nearly zero. This means that the conversion rate is no longer dependent on the degrees of coverage, but maybe on the vicinity of the adsorbed methanol on the surface. This vicinity of two adsorbed methanol molecules results from the fact that the products are removed from the surface first.

Another representation of the same results is shown in Fig. 6. All curves at increased pressures (higher methanol concentration) approach a limit value that corresponds to the complete coverage of the active centres on the surface.

Our experiments were carried out in exactly this area. This means that the surface was covered completely from the very beginning, among others with H_2O that always exists as an impurity, but also with N_2, Ar, and He that slowly had to be replaced by methanol.

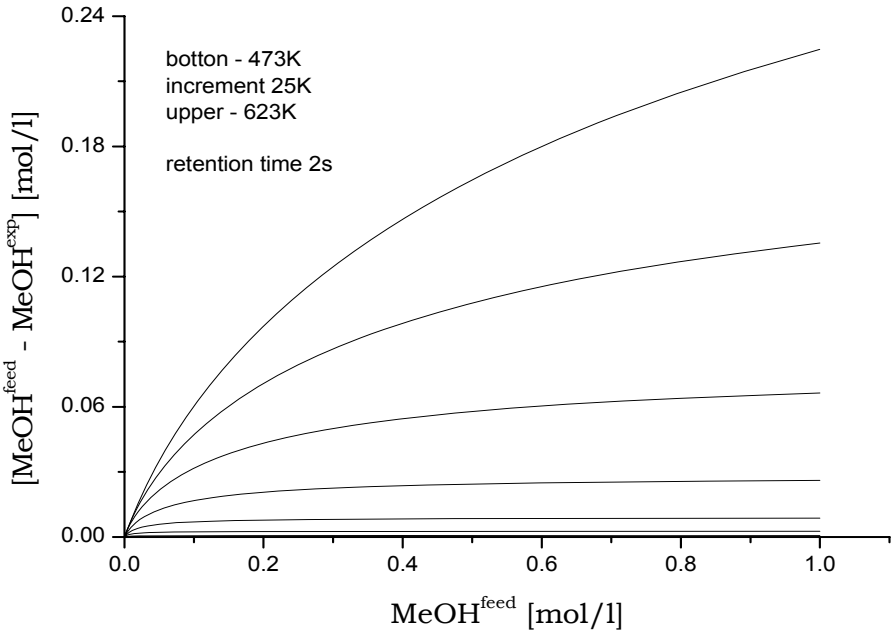

Fig. 6. Methanol concentration as a function of the increasing concentration in the feed gas.

Model calculation, now with the total of the error squares being ($2.19*10^{-5}$), also yielded the values for the rate constants of the individual reactions as well as the activation energies of the reactions included in the model. The calculated values are listed in Table 6.

Table 6. Optimal kinetic parameters k^0_i and E_i of the elementary reaction mechanisms given in Table 5

Units	k^0_i	E_i / kJ	Reaction
s^{-1}	$k_1 = 7.94.10^{10}$	0	$CH_3OH + Z$ ------> CH_3OH^{ads}
mol/l.s	$k_4 = 7.94.10^{13}$	61	CH_3OH^{ads} ------> $CH_3OH + Z$
s^{-1}	$k_2 = 4.68.10^{09}$	0	$DME + Z$ ------> DME^{ads}
mol/l.s	$k_5 = 3.63.10^{07}$	37	DME^{ads} ------> $DME + Z$
s^{-1}	$k_3 = 1.58.10^{12}$	0	$H_2O + Z$ ------> H_2O^{ads}
mol/l.s	$k_6 = 1.78.10^{08}$	24	H_2O^{ads} ------> $H_2O + Z$
mol/l.s	$k_7 = 8.32.10^{07}$	106	$CH_3OH^{ads} + CH_3OH^{ads}$ ------> $DME^{ads} + H_2O^{ads}$
mol/l.s	$k_8 = 1.00.10^{12}$	137	$DME^{ads} + H_2O^{ads}$ ------> $CH_3OH^{ads} + CH_3OH^{ads}$

It is surprising that the desorption heat of methanol in the table above exceeds that of H_2O. It amounts to 61 kJ/mol and, hence, is far in the “chemisorption range“. Consequently, the inelastic neutron scattering experiments (INS) and infrared spectroscopy (IR) of methanol adsorbed on η–alumina as performed by A. McInroy and *co-workers* [21] experimentally confirmed the splitting of CH_3OH into a negative CH_3O^- and a positively bound H^+ as

postulated by Bandiera [16]. This means that the adsorbed methanol exists in a quasi “ionic state” and, hence, bonding with this substrate is stronger. This finding is reflected by the adsorption energy of methanol exceeding that of the other components.

Finally, to test the influence of the reactor type on the kinetics, the results obtained with the same kinetic model for a flow-type reactor and a stirring reactor were compared. Of course, the data sets varied, but this did not affect the kinetics. For the experiments presented here, the flow-type reactor was used.

To sum up, it can be concluded that the experimental results are reproduced well by the Hinshelwood kinetics on the basis of elementary reactions. The resulting desorption energy for methanol can be explained by an “ionic bonding” with the active centre.

3. Literature

[1] Ki-Won Jun; Hye-Soon Lee; Hyun-Seog Roh and Sang-Eon Park. Catalytic Dehydration of Methanol to DME over Solid-Acid Catalysts. Bull. Korean Chem. Soc. 2002, Vol. 23, No. 6. 803-806.

[2] S. Jiang, J-S Hwang; T. Jin, S-E. Park. Dehydration of Methanol to Dimethyl Ether over ZSM-5 Zeolite. Bull. Korean Chem. Soc. 2004, Vol. 25, No. 2. 185-189.

[3] Jun; Lee; Park. Highly water-enhanced H-ZSM-5 catalysts for dehydration of methanol to DME. Bull. Korean. Chem. Soc. 2003, Vol. 24, No. 1. 106-108.

[4] F. Yaripour ; F. Baghaei ; I. Schmidt ; J. Perregaard. Catalytic dehydration of methanol to dimethyl ether (DME) over solid-acid catalysts. Catalysis Communications 6 (2005) 147-152.

[5] M. Hirano; T. Imai; T. Yasutake and K. Kuroda. Dimethyl Ether Synthesis from Carbon Dioxide by Catalytic Hydrogenation (Part1). Activities of Methanol Dehydration Catalysts. Journal of Japan Petroleum Institute, 45 (3). 169-174 (2002).

[6] V. Vishwanathan; K-W. Jun; J-W. Kim; H-S Roh. Vapour phase dehydration of crude methanol to dimethyl ether over Na-modified H-ZSM-5 catalysts. Applied Catalysis A: General 276 (2004) 251-255.

[7] Oh-Shim Joo; Kwang-Deog Jung and Sung-Hwan Han. Modification of H-ZSM-5 and γ-Alumina with Formaldehyde and Its Application to the Synthesis of Dimethyl Ether from Syn-gas. Bull. Korean. Chem. Soc. 2002, Vol. 23, No. 8. 1103-1105.

[8] M. Xu; J. H. Lunsford; D. W. Goodman; A. Bhattacharyya. Synthesis of dimethyl ether (DME) from methanol over solid-acid catalysts. Applied Catalysis A: General 149 (1997) 289-301.

[9] S. Jiang; Y. K. Hwang, S.-H. Jhung; J.S. Chang; J.-S. Hwang; T. Cai and S.-E. Park. Zeolite SUZ-4 as Selective Dehydration Catalyst for Methanol Conversion to Dimethyl Ether. Chemistry Letters Vol. 33, No. 8 (2004) 1048-1049.

[10] Grigore Pop; Cristian Theodorescu. SAPO-34 Catalyst For Dimethylether Production. Studies in Surface Science and Catalysis 130, 287-292. 2000 Elsevier Science B. V.

[11] Michael G. Abraha; Xianchun Wu and Rayford G. Anthony. Effects of Particle Size and Modified SAPO-34 on Conversion of Methanol to Light Olefins and Dimethyl Ether. Studies in Surface Science and Catalysis 133, 211-218. 2001 Elsevier Science B. V.

[12] Xianchun Wu; Michael G. Abraha; Rayford G. Anthony. Methanol conversion on SAPO-34: reaction condition for fixed-bed reactor. Applied Catalysis A: General 260 (2004) 63-69.

[13] V. Vishwanathan; H.-S. Roh; J.-W. Kim and Ki-Won Jun. Surface properties and catalytic activity of TiO_2-ZrO_2 mixed oxides in dehydration of methanol to dimethyl ether. Catalysis Letters Vol. 96, Nos. 1-2, July 2004, 23-28.

[14] Henry P. Pinto, R. M. Nieminen, and Simon D. Eliott. Ab initio of γ-Al_2O_3 surfaces. Physical Review 70, 125402 (2004), 1-11.

[15] E. A. Kotomin and A. I. Popov, Nucl. Instrum. Methods Phys. Res. B 141, 1 (1998).

[16] Jean Bandiera and Claude Naccache. Kinetics of methanol dehydration on dealuminated H-mordenite: Model with acid and basic active centres. Applied Catalysis, 69 (1991) 139-145.

[17] Ludmila Kubelková, Jana Nováková, and Kvéta Nedomová. Reactivity of Surface Species on Zeolites in Methanol Conversion. Journal of Catalysis 124, 441-450 (1990).

[18] Solange R. Blaszkowski and Rutger A. van Santen. The Mechanism of Dimethyl Ether Formation from Methanol Catalyzed by Zeolitic Protons. J. Am. Chem. Soc. 1996, 118, 5152-5153.

[19] Gorazd Bercic and Janez Levec. Intrinsic and Global Reaction Rate of Methanol Dehydration over γ-Al_2O_3 Pellets. Ind. Eng. Chem. Res. 1992, 31, 1035-1040.

[20] H. J. Ederer; T. Fritsch; E. Henrich; C. Mas. Kinetics of the Water-Gas Shift Reaction Using *MoS_2* Catalyst Dotted with *Co*. Wissenschaftliche Berichte FZKA 6761. (October, 2002). Forschungszentrum Karlsruhe. In English.

[21] Alastair Mcluroy, John Winfield, Cris Dudman. An infrared and inelastic neutron scattering spectroscopic investigation on the interaction of η-alumina and methanol. Research paper, Phys. Chem. Chem.Phys. 2005, 7, 3093-3101.

Acknowledgements

We are very thankful to Mr. Kahrau, Mr. Meinzer and Mr. Kehrwecker who supported us in planning and constructing the electronical devices and the whole gadgetry.